Anal. Chem. **1997,** *69,* 5109−5120

Frequency Domain Multidimensional Fluorescence: A Route to Model-Independent Fluorescence Decay Analysis

Sharon L. Neal

Department of Chemistry, University of California at Riverside, Riverside, California 92521

A multivariate method for analyzing complex fluorescence decays without model assumptions is described. This method is applicable to the decays of mixtures of spectrally distinct fluorophores. The method does not require specific information concerning the component spectra or lifetimes, but such information can be used when it is available. The decay is analyzed as the complex quantum yield (a function of the steady-state intensity, modulation ratio, and phase angle) measured as a function of modulation frequency and, in most cases, emission wavelength. When the spectra of the mixture components are known, the frequency domain decays of the components can be calculated from complex quantum yield matrices measured at all or selected wavelengths. Matrices describing component photokinetics and relative concentrations are calculated from the frequency domain decays. When the component emission spectra are not known, complex quantum yield matrices can be factored into the emission spectra and frequency domain decays of the sample components via principal components analysis of the matrix. In this paper, the principles of frequency domain decay analysis are discussed. In particular, the variation of the analysis procedure with the amount of data acquired and the extent of the analyst's knowledge of the sample components are described. These procedural variations are illustrated by the analysis of simulated decays and the decays of mixtures of polynuclear aromatic hydrocarbons in isotropic and microheterogeneous solution.

Due to the similarity of the excited-state lifetime of many fluorophores and the time scale of molecular motion, time-dependent measurements of fluorescence probes are widely used to characterize binding sites in biological molecules[1] and solubilization sites in organized media[2] and to monitor molecular dynamics.[3] One of the limitations the analyst must address in order to exploit this capacity is the inherent ambiguity in the analysis of complex fluorescence decays. Several approaches to analyzing fluorescence decays in the time and frequency domain have been developed. Most often, the experimental decay is fit to combinations of monoexponential decays, or distributions of decays, via nonlinear least squares.[4,5] This approach is very general; the analyst can fit the data to a wide variety of prospective photokinetic models including multistep excited-state reactions. The limitation of this approach is the subjectivity inherent in fitting experimental data to photokinetic models and the resultant ambiguity in the analysis results. This ambiguity can be reduced by global, i.e., linked, least-squares fitting analysis of frequency domain decays measured under systematically varied conditions, but the subjectivity inherent in photokinetic model selection remains.[6] It has been shown that most multiexponential decays can be described as a combination of three monoexponentials and that extremely precise data are required to distinguish combinations of discrete decays from decays characterized by distributions of decay constants.[7]

Earlier research into the analysis of fluorescence decays has produced methods that avoid the subjectivity and ambiguity of parametric analyses in specific instances. Distributed decays can be analyzed without a priori assumptions regarding the shape of the distribution by the maximum entropy method (MEM).[8,9] Excimer decay times can be analyzed with minimal assumptions via the β method when the monomer decay time is known.[10] The convolution method can be used to analyze the decay times of species involved in excited-state reactions if the number of species is known.[11] Clearly, none of the aforementioned methods match the general applicability of the least-squares fitting approach.

Recently, a more general model-independent approach to the analysis of multicomponent fluorescence decays has been developed. It has been demonstrated that it is possible to analyze multidimensional, i.e., wavelength-resolved, decays in the frequency domain without model assumptions,[12] even if the mixture components are participating in excited-state reactions[13] because the Fourier coefficients of the decay are linearly related to the photokinetic transfer matrix describing the time evolution of the excited-state species.[14] This development has two important benefits. First, the results are less susceptible to bias on the part of the analyst. Second, since multidimensional decays are simultaneously partitioned into component spectra as well as decays, the lifetimes and photokinetic mechanism indicated by the decays are corroborated by emission spectra. This develop-

(1) Sytnik, A.; Gormin, D.; Kasha, M. *Proc. Natl. Acad. Sci. U.S.A.* **1994**, *91*, 11968−11972.
(2) Tocanne, J. F.; Pérochon, E.; Lopez, A. *Biochemistry* **1992**, *31*, 7672−7682.
(3) Davenport, L.; Targowski, P. *Biophys. J.* **1996**, *71*, 1837−1852.
(4) Gratton, E.; Limkeman, M.; Lakowicz, J. R.; Laczko, G.; Cherek, H. *Biophys. J.* **1984**, *46*, 463−477.
(5) Gratton, E.; Alcala, J. R.; Prendergast, F. G. *Biophys. J.* **1987**, *51*, 587−596.
(6) Lofroth, J. E. *J. Phys. Chem.* **1986**, *90*, 1160−1168.
(7) James, D. R.; Ware, W. R. *Chem. Phys. Lett.* **1986**, *126*, 7−11.
(8) Brochon, J.-C.; Livesey, A. K. *Biophys. J.* **1987**, *52*, 693−706.
(9) Brochon, J.-C.; Livesey, A. K.; Pouget, J.; Valeur, B. *Chem. Phys. Lett.* **1990**, *174*, 517−522.
(10) Duhamel, J.; Yekta, A.; Winnik, M. A. *J. Phys. Chem.* **1993**, *96*, 2759−2763.
(11) Pansu, R. B.; Yoshihara, K.; Arai, T.; Tokumaru, K. *J. Phys. Chem.* **1993**, *97*, 1125−1133.
(12) Neal, S. L. *J. Phys. Chem.* **1997**, *101*, 6883−6889.
(13) Villegas, M. M.; Neal, S. L. *J. Phys. Chem.* **1997**, *101*, 6890−6896.
(14) Sugar, I. P. *J. Phys. Chem.* **1991**, *95*, 7508−7515.

S0003-2700(97)00321-1 CCC: $14.00

ment substantially reduces the ambiguity associated with the analysis of systems comprised of three or more fluorescent decays.

In contrast to the earlier work on model-free decay analysis, this paper focuses on the analysis of mixture decays that do not exhibit excited-state reactions. The objective of this work is to survey the variation of frequency domain analysis procedures and results with the amount of data acquired and the extent of the analyst's knowledge of the sample components. If the fluorescence decay is measured across the entire mixture emission spectrum, the component decays can be analyzed without a priori knowledge of the component spectra. However, quantitative analysis in this instance does require knowledge of the relative quantum yields of the components. On the other hand, in order to analyze fluorescence decays measured at selected wavelengths (the number of wavelengths must equal or exceed the number of spectral components), the analyst must have the emission spectra of component standards, i.e., the relative intensities of component standards, at the selected wavelengths. Since these data reflect the relative quantum yields of the components, the relative concentrations of the mixture components also can be determined.

In the Theory section, the principles of the analysis are derived briefly and the procedural variations on the analysis are described. These procedures are described in order of increasing complexity, i.e., from the analysis of single-wavelength−single-component decay to the analysis of multicomponent decay matrices without a priori knowledge of the spectra. The Results and Discussion section begins with an analysis of the frequency domain decay of a single fluorophore. The raw data and graphical illustration of the analysis residuals are presented for this simplest example. This section is followed by the description of the analysis of simulated and, then, experimental decays. The simulations are used to compare the impact of the various procedures on the analysis results. The experimental decays, acquired from mixtures of polynuclear aromatic hydrocarbons (PAHs), also were analyzed using a range of analysis procedures. The analyses of the experimental decays also illustrate the impact of low signal-to-noise ratio (SNR) and component response overlap on the results frequency domain decay analysis. However, the systematic evaluation of the impact of the SNR, spectral overlap, and temporal overlap on all the variations of the analysis procedure is beyond the scope of this paper.

Research on the resolution of mixtures by analysis of wavelength-dependent frequency domain decays is related to, but different from, the frequency domain analysis method presented here. The analysis of the decay kinetics is usually not the goal of these mixture analyses. The most developed approach is based on solving systems of simultaneous equations constructed from phase-resolved fluorescence intensities (PRFIs).[15−18] Mixtures can also be analyzed by global analysis of decays measured as a function of emission wavelength.[19] As discussed previously, the photokinetics are analyzed using this approach, but the analyst is required to select a model for the photokinetic mechanism.

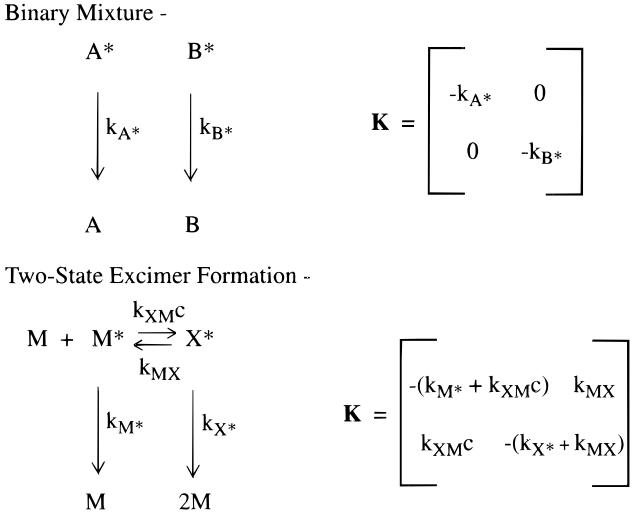

Figure 1. Photokinetic mechanisms and transfer matrices of a binary noninteracting, i.e., ground-state heterogeneous, mixture and a two-state excimer formation, i.e., Birks model, reaction.

The following notation is used throughout this paper. Matrices are denoted by uppercase, boldface Roman and Greek letters. Vectors are denoted by lowercase, boldface Roman and Greek letters. Vectors that are columns of a matrix are denoted using the subscripted, boldface matrix variable, i.e., $\mathbf{m}_j$ denotes the jth column of **M**. Similarly, vectors that are rows of the matrix **M**, are denoted $\mathbf{m}_{i,}$ where i represents the ith row. Of course, the matrix element on row i in column j is denoted m_{ij}. Scalars that are not drawn from matrices and vectors are denoted by lowercase, italic Roman and Greek letters. Complex variables are indicated using a superpositioned tilde, i.e., $\tilde{\mathbf{M}}$ and its complex conjugate is denoted using a superscripted asterisk, $\tilde{\mathbf{M}}^*$. As usual, superscript −1 denotes the matrix inverse, the slanted prime (′), denotes the matrix transpose, a superpositioned bar, e.g., $\bar{\mathbf{M}}$, indicates the column average and double vertical bars, ||**m**||, indicate the length of the designated vector, i.e., the square root of the sum of the squares of the vector elements. The function diag(**M**) extracts the diagonal of the designated matrix as a vector and expands designated vectors, i.e., diag(**m**), into matrices that have **m** on the diagonal.

THEORY

Frequency Domain Decays. The basis of nonparametric frequency domain analysis is the linear relationship between the derivative of a frequency domain decay and the photokinetic transfer matrix governing the time evolution of excited-state species. The derivation of the method from this relationship has been discussed fully elsewhere and is only summarized here.[12] When the kinetic equations governing the decay of n excited-state fluorophores are written as a system of coupled first-order differential equations, i.e.

$$d\mathbf{y}/dt = \mathbf{K}\mathbf{y} + \mathbf{e} \qquad (1)$$

the $n \times n$ coefficient matrix, **K**, describes the decay and interaction of the excited-state molecules, the instantaneous concentration of the excited-state species are stored in the $n \times 1$ vector **y**, and **e** is the n-component excitation function. In time domain decay measurements, the components of **e** are ideally Dirac functions. The diagonal elements of the matrix **K** are the decay rates, i.e.,

(15) Bright, F. V.; McGown, L. B. *Anal. Chem.* **1984**, *56*, 1400A−1412A.
(16) Millican, D. W.; McGown, L. B. *Anal. Chem.* **1989**, *61*, 580−583.
(17) Burdick, D. S.; Tu, X. S.; McGown, L. B.; Millican, D. W. *J. Chemom.* **1990**, *4*, 15−29.
(18) McGown, L.; Millican, D. W. *Anal. Chem.* **1990**, *62*, 2242−2247.
(19) Lakowicz, J. R.; Jayaweera, R.; Szmacinski, H.; Wiezk, W. *Anal. Chem.* **1990**, *62*, 2005−2012.

negative inverse excited-state lifetimes, of the sample components. The off-diagonal elements are the rates of excited-state reactions between the components. In this paper, **K** will be called the photokinetic transfer matrix. Figure 1 depicts the photokinetic mechanisms and transfer matrices corresponding to a noninteracting mixture, i.e., a ground-state heterogeneous mixture, and a system undergoing a two-state (Birks) excimer formation reaction.[20]

Since taking the Fourier transform of a function derivative is equivalent to multiplying the function transform by the complex frequency, the Fourier transform coefficients of the emission decay at a single frequency, $\tilde{\mathbf{y}}$, are linearly related to the photokinetic transfer matrix. Specifically,

$$\frac{\mathrm{d}\tilde{\mathbf{y}}}{\mathrm{d}t} = \mathbf{K}\tilde{\mathbf{y}} = \iota\omega\tilde{\mathbf{y}} - \mathbf{y}_0 \tag{2}$$

where the components of $\tilde{\mathbf{y}}$ are the Fourier transform coefficients of the decays at frequency ω and the components of $\mathbf{y}_0$ are the initial intensities of the time domain decays.[14] The frequency domain decay components, $\tilde{\mathbf{y}}$, can be measured experimentally by Fourier transformation of time-resolved decays or calculation from the modulation ratio and phase shift acquired from phase-resolved decays generated by use of sinusoidally modulated excitation light. The modulation ratio and phase shift are related to the real and imaginary components of the frequency domain decay through the following expressions:

$$\tilde{\mathbf{y}}_{\mathrm{real}} = \mathbf{\Lambda}(\mathbf{m}\odot\cos\phi) \qquad \tilde{\mathbf{y}}_{\mathrm{imag}} = \mathbf{\Lambda}(\mathbf{m}\odot\sin\phi) \tag{3}$$

$$\tilde{\mathbf{y}} = \tilde{\mathbf{y}}_{\mathrm{real}} + \iota\tilde{\mathbf{y}}_{\mathrm{imag}} \tag{4}$$

where $\mathbf{\Lambda}$ is a diagonal matrix of component decay constants, **m** is a vector of component modulation ratios, ϕ is a vector of component phase shifts (angles), and $\odot$ denotes element by element multiplication. The vectors $\tilde{\mathbf{y}}_{\mathrm{real}}$ and $\tilde{\mathbf{y}}_{\mathrm{imag}}$ contain the real and imaginary Fourier coefficients, respectively, of the n decay components.

When the frequency domain decay is measured at q excitation modulation frequencies, eq 2 can be expanded to

$$\mathbf{K}\tilde{\mathbf{Y}}' = \tilde{\mathbf{Y}}'\tilde{\mathbf{\Omega}} - \mathbf{Y}'_0 \tag{5}$$

where $\mathbf{\Omega}$ is a diagonal $q \times q$ matrix of complex modulation frequencies and $\mathbf{Y}_0$ is a $q \times n$ matrix that has identical rows comprised of the initial intensities of the n time domain decays. As a result of this relationship, the photokinetics of *any* system governed by coupled first-order linear differential equations with constant coefficients can be determined from the component frequency domain decays, i.e., the columns of $\tilde{\mathbf{Y}}$, without fitting. The photokinetic matrix is the unknown in an overdetermined system of equations formed by the imaginary part of eq 5. Therefore **K** can be determined using the following expression:

$$\mathbf{K} = (\tilde{\mathbf{Y}}'\tilde{\Omega})_{\mathrm{imag}}(\tilde{\mathbf{Y}}'_{\mathrm{imag}})^{+} \tag{6}$$

where the subscript imag refers to the imaginary part of the matrix and superscript + denotes the pseudoinverse. The pseudoinverse[21] of a matrix is used to solve linear systems when the coefficient matrix, here $\tilde{\mathbf{Y}}_{\mathrm{imag}}$, is not square and thus has no inverse. Since $\tilde{\mathbf{Y}}^{+}_{\mathrm{imag}}\tilde{\mathbf{Y}}_{\mathrm{imag}} = \mathbf{I}$, the pseudoinverse solves the system of equations in spite of the structural deficiencies of $\tilde{\mathbf{Y}}_{\mathrm{imag}}$. The pseudoinverse calculates the solution with the shortest length of the infinite number of system solutions. The pseudoinverse is calculated from the singular value decomposition of a matrix: $\tilde{\mathbf{Y}}_{\mathrm{imag}} = \tilde{\mathbf{U}}\tilde{\mathbf{\Sigma}}\tilde{\mathbf{V}}'$; $\tilde{\mathbf{Y}}^{+}_{\mathrm{imag}} = \tilde{\mathbf{V}}\mathbf{\Sigma}^{-1}\tilde{\mathbf{U}}'$, where $\tilde{\mathbf{U}}$ and $\tilde{\mathbf{V}}$ are orthonormal basis vectors for the columns and rows of the matrix, respectively, and $\mathbf{\Sigma}$ is a diagonal matrix whose elements reflect the contribution of the product of the corresponding basis vectors to the total variance of the matrix. The initial intensity matrix can be calculated by rearrangement of eq 5:

$$\mathbf{Y}'_0 = \tilde{\mathbf{Y}}'\tilde{\mathbf{\Omega}} - \mathbf{K}\tilde{\mathbf{Y}}' \tag{7}$$

Since the rows of this matrix are ideally identical, any row contains the n initial intensity values. In analyses of experimental data, the average or mode across rows of $\mathbf{Y}_0$ will yield the initial intensity values. Experimental intensities are scaled by the time domain sampling interval and instrumental factors, so it is convenient to report fractional or relative intensities.

Single-Component Decays. In some cases, e.g., lifetime determination of standard solutions, the analyst has a high degree of confidence that the emission decay is monoexponential. The decay can be measured at a single emission wavelength or through a filter that blocks scattered excitation light. It is possible to calculate the lifetime of such decays using single-component versions of eqs 6 and 7. In this case, the normalized complex quantum yield vector, $\tilde{\mathbf{d}}^{\ddagger}$, is calculated from the phase angle and modulation ratio measured at the various modulation frequencies: $\tilde{\mathrm{d}}^{\ddagger}(\omega) = \mathrm{m}(\omega)\mathrm{e}^{\iota\phi(\omega)}$. The decay constant is calculated using the following variant of eq 5:

$$k = (\tilde{\mathbf{d}}^{\ddagger}\tilde{\mathbf{\Omega}})_{\mathrm{imag}}\frac{(\tilde{\mathbf{d}}^{\ddagger}_{\mathrm{imag}})'}{||\tilde{\mathbf{d}}^{\ddagger}_{\mathrm{imag}}||} \tag{8}$$

where the subscript imag refers to the imaginary part of the normalized complex quantum yield vector. All the elements of the zero time response vector, which is given by $\mathbf{d}^{\ddagger}_0 = \tilde{\mathbf{d}}^{\ddagger}\tilde{\mathbf{\Omega}} - k\,\tilde{\mathbf{d}}^{\ddagger}$, will equal the same value, within experimental variation, when the decay is indeed monoexponential.

Frequency Domain Emission-Decay Matrix. When the fluorescence decay of a mixture of n fluorophores is measured as a function of emission wavelength in the frequency domain, the emission decay at the various wavelengths can be arranged into $p \times q$ matrix, $\tilde{\mathbf{D}}$, where p is the number of emission wavelengths monitored and q is the number of modulation frequencies used to sample the decay. The decay profiles of individual mixture components are independent of the emission wavelength; therefore, the matrix $\tilde{\mathbf{D}}$ is the sum of the outer products of the digitized emission spectra and frequency domain decays of the components. This relationship is expressed mathematically in the expression

(20) Birks, J. B.; Dyson, D. J.; Munro, I. H. *Proc. R. Soc. A* **1963**, *275*, 575−588.

(21) Strang, G. *Introduction to Applied Mathematics*; Wellesley-Cambridge Press: Wellesley, MA, 1986.

$$\tilde{\mathbf{D}} = \sum_{k=1}^{n} \mathbf{x}_{\bullet k}\, \tilde{\mathbf{y}}'_{\bullet k} = \mathbf{X}\tilde{\mathbf{Y}}' \tag{9}$$

where the columns of the $p \times n$ matrix $\mathbf{X}$, $\mathbf{x}_{\bullet k}$, are the time-independent emission spectra of the n components and the columns of the $q \times n$ matrix $\tilde{\mathbf{Y}}$, $\tilde{\mathbf{y}}_{\bullet k}$, are the frequency domain decays of the n components. The normalization of $\mathbf{X}$ is critical, the columns of $\mathbf{X}$ should be proportional to the product of the molar absorptivity, ϵ, and photon emission rate, k_F, of each component. In this paper, this product will be called the photon production rate.

Each element of $\tilde{\mathbf{D}}$ is a complex quantum yield value[14] calculated from the steady-state emission intensity, phase shift, and modulation factor as follows,

$$\tilde{d}(\lambda,\omega) = s(\lambda,0)m(\lambda,\omega)e^{\iota\phi(\lambda,\omega)} \tag{10}$$

In this expression, $\tilde{d}(\lambda,\omega)$ is the frequency domain response at wavelength λ and frequency ω (the λth, ωth element of the complex quantum yield matrix, $\tilde{\mathbf{D}}$), $s(\lambda,0)$ represents the intensity of the steady-state emission spectrum of the sample at wavelength λ, $m(\lambda,\omega)$ is the modulation factor, and $\phi(\lambda,\omega)$ is the phase shift at wavelength λ and modulation frequency ω. The time-independent emission spectrum, $\mathbf{x}$, is the steady-state emission spectrum, $\mathbf{s}$, scaled by the fluorophore lifetime, i.e., $\mathbf{s} = \mathbf{x}\tau$.

Multicomponent Decays. The key to analysis of multicomponent frequency domain decays is the resolution of the component decays from the mixture decay so that the decay constants can be calculated via eq 6. When the emission spectra are known, they can be used to calculate the component decays from the decay matrix of mixtures. In the case that the analyst has no a priori information concerning the sample components, the component decays are determined by factoring the frequency domain emission-decay matrix of the mixture into the constituent component spectra and decays.

Matrix Acquisition/No a priori Information. In the case that the analyst has no a priori information concerning the number or spectra of the sample components, mixture decays can be analyzed by partitioning the complex quantum yield matrix into the spectra and frequency domain decays of the components via principal components analysis and a variant[22] of self-modeling curve resolution.[23] The procedure is recounted here briefly. Further details of this method are described elsewhere.[12,13]

Any matrix $\tilde{\mathbf{D}}$ can be factored into principal components:

$$\tilde{\mathbf{D}} = \tilde{\mathbf{U}}\tilde{\mathbf{Q}}' \tag{11}$$

where the columns of the $p \times m$ matrix $\tilde{\mathbf{U}}$ are complex, orthonormal ($\tilde{\mathbf{U}}'\tilde{\mathbf{U}} = \mathbf{I}$) basis vectors for the column space of $\tilde{\mathbf{D}}$, the columns of the $q \times m$ matrix $\tilde{\mathbf{Q}}$ are complex, orthogonal ($\tilde{\mathbf{Q}}'\tilde{\mathbf{Q}} = \mathbf{\Sigma}$; from the singular value decomposition of $\tilde{\mathbf{D}} = \tilde{\mathbf{U}}\Sigma\tilde{\mathbf{V}}'$) basis vectors for the row space of $\tilde{\mathbf{D}}$ and m is the smaller of the two matrix dimensions p and q. The number of basis vectors is equal to m rather than n due to the superposition of measurement noise on the decay signal. However, only n of these basis vectors are required to describe the variance associated with the spectral signal. The remaining $m-n$ vectors describe noise and should be eliminated from the matrices $\tilde{\mathbf{U}}$ and $\tilde{\mathbf{Q}}$ prior to further analysis. When the number of fluorescent components is not known prior to the analysis, n can be estimated by a number of statistical and signal processing methods.[13,24,25] From this point, $\tilde{\mathbf{U}}$ and $\tilde{\mathbf{Q}}$ are considered to be $p \times n$ and $q \times n$ matrices, respectively.

The data matrix $\tilde{\mathbf{D}}$ is the product of $\tilde{\mathbf{U}}$ and $\tilde{\mathbf{Q}}$, but these basis vectors lack the mathematical features of spectra and decays. The spectral vectors, the columns of $\mathbf{X}$, must be real and nonnegative. The columns of $\tilde{\mathbf{U}}$ meet neither of these conditions. When subjected to eqs 6 and 7, the frequency domain decays, the columns of $\tilde{\mathbf{Y}}$, yield real, nonnegative initial intensities, $\mathbf{Y}_0$, that have the same values for all frequencies and diagonal $\mathbf{K}$ matrices with negative diagonal elements. The columns of $\tilde{\mathbf{Q}}$ do not meet these requirements either. $\mathbf{X}$ can be reconstructed from $\tilde{\mathbf{U}}$ by combining multiples of the columns of $\tilde{\mathbf{U}}$ so that they form vectors that meet the mathematical conditions on spectra. The matrix $\tilde{\mathbf{Y}}$ is similarly reconstructed from $\tilde{\mathbf{Q}}$, but with the additional constraint that the product of $\mathbf{X}$ and $\tilde{\mathbf{Y}}$ continue to equal $\tilde{\mathbf{D}}$. This is accomplished via transformation matrix $\tilde{\mathbf{I}}\tilde{\mathbf{I}}$:

$$\tilde{\mathbf{D}} = \tilde{\mathbf{U}}\tilde{\mathbf{I}}\tilde{\mathbf{I}}\tilde{\mathbf{I}}^{-1}\tilde{\mathbf{Q}}' = \mathbf{X}\tilde{\mathbf{Y}}' \tag{12}$$

$$\mathbf{X} = \tilde{\mathbf{U}}\tilde{\mathbf{I}}\tilde{\mathbf{I}} \tag{13}$$

$$\tilde{\mathbf{Y}} = \tilde{\mathbf{Q}}(\tilde{\mathbf{I}}\tilde{\mathbf{I}}^{-1})' \tag{14}$$

The values of $\tilde{\mathbf{I}}\tilde{\mathbf{I}}$ that accomplish this transformation are determined by nonlinear optimization. The objective function is the length of the vector that has elements calculated from the deviations of $\tilde{\mathbf{U}}\tilde{\mathbf{I}}\tilde{\mathbf{I}}$ and $\tilde{\mathbf{Q}}(\tilde{\mathbf{I}}\tilde{\mathbf{I}}^{-1})'$ from the required structure of $\mathbf{X}$ and $\tilde{\mathbf{Y}}$. Specifically, the elements of the objective function vector are the negative and complex values of $\tilde{\mathbf{U}}\tilde{\mathbf{I}}\tilde{\mathbf{I}}$, the negative and complex values of $\mathbf{Y}_0$, positive diagonal elements, and nonzero off-diagonal elements of $\mathbf{K}$ calculated from $\tilde{\mathbf{Q}}(\tilde{\mathbf{I}}\tilde{\mathbf{I}}^{-1})'$. A scaled χ^2 value (very large values will complicate the optimization), calculated using idealized versions of $\mathbf{X}$, $\mathbf{K}$, and $\mathbf{Y}_0$ (i.e., infeasible values deleted) can also be an element of the objective function vector. As these elements are reduced, the length the objective function vector approaches zero and $\tilde{\mathbf{U}}\tilde{\mathbf{I}}\tilde{\mathbf{I}}$ and $\tilde{\mathbf{Q}}(\tilde{\mathbf{I}}\tilde{\mathbf{I}}^{-1})'$ are reconciled to the mathematical constraints on spectra and decays and transforming them to $\mathbf{X}$ and $\tilde{\mathbf{Y}}$. The accuracy of the transformation depends on several factors including the signal-to-noise ratio (S/N) of the data, the similarity of the component spectra and decay profiles, and the number of nonzero off-diagonals in $\mathbf{K}$. Accurate transformations are promoted by high S/N, dissimilar spectra and lifetimes, and diagonal $\mathbf{K}$ matrices. The photokinetic transfer matrix and initial intensities can be calculated from the reconstructed frequency domain decays using eqs 6 and 7, respectively.

Equation 5 does not reveal all of the structural details of the component decays. These decays are combinations of the unit exponential decays. The nature of the photokinetic matrix $\mathbf{K}$ determines how the unit exponentials are combined in component decays. This is illustrated in an alternative expression for the decay given by

(22) Neal, S. L.; Davidson, E. R.; Warner, I. M. *Anal. Chem.* **1990**, *62*, 658−664.
(23) Lawton, W. H.; Sylvestre, E. A. *Technometrics* **1971**, *13*, 617−633.
(24) Wold, S. *Technometrics* **1978**, *20*, 397−405.
(25) Shrager, R. I.; Hendley, R. W. *Anal. Chem.* **1982**, *54*, 1147−1152.

$$\tilde{\mathbf{Y}}' = \mathbf{W}\Gamma\tilde{\mathbf{Z}}' \quad (15)$$

where the unit frequency domain decays are stored along the columns of the $q \times n$ matrix $\tilde{\mathbf{Z}}$. The matrix $\mathbf{W}$ has columns that are the eigenvectors of the transfer matrix $\mathbf{K}$ and combines the unit decays into the component decays. The diagonal elements of the $n \times n$ matrix $\mathbf{\Gamma}$ are concentration-dependent factors, given by $\mathbf{W}^{-1}\mathbf{y}_0$. When there is no excited-state reaction complicating the decay of a mixture, $\mathbf{K}$ is a diagonal matrix, making $\mathbf{W}$ the identity matrix and the component decays single exponentials.

In the case of noninteracting fluorophores whose decays are described by distributions of rates, the complex quantum yield matrix is given by

$$\tilde{\mathbf{D}} = \mathbf{X}\mathbf{G}\Gamma\tilde{\mathbf{Z}}' = \mathbf{X}\bar{\tilde{\mathbf{Y}}}' \quad (16)$$

where the matrix $\mathbf{G}$, is an $n \times nd$ matrix of ones and zeros which combines all the decays that emit a given spectrum and the definitions of $\tilde{\mathbf{Y}}$, $\mathbf{\Gamma}$, and $\tilde{\mathbf{Z}}$ are unchanged but their sizes have been expanded to $nd \times nd$ and $q \times nd$, respectively, to reflect the increase in the number of decay rates. In this case, the results of frequency domain analysis are $\mathbf{X}$, $\mathbf{GKG}^+$, and $\mathbf{Gy}_0$. Since $\mathbf{G}$ averages the rows of $\bar{\tilde{\mathbf{Y}}}$ that correspond to the same spectra, the values of $\mathbf{GKG}^+$ and $\mathbf{Gy}_0$ correspond to the mean properties of distributed decays. Each column of $\bar{\tilde{\mathbf{Y}}}$ is the combined decay of all the excited states that emit the corresponding spectrum. This combined decay is characterized by a distribution of decay constants. The relative contribution of each unit decay to the distributed, i.e., combined, decay is described by the fluorescence lifetime distribution, $\mathbf{f}_k$ of the decay. The distribution is given by the expression

$$\bar{\tilde{\mathbf{y}}}_k = \sum\nolimits_i \mathrm{f}_{ik}\tilde{\mathbf{z}}_i \quad (17)$$

The lifetime distribution, $\mathbf{f}$, for each component decay, can be estimated nonparametrically from the distributed frequency domain decay, $\bar{\tilde{\mathbf{y}}}$, by subjecting it to the inverse Fourier and Laplace transformations using the MEM.[9,26] Shaver and McGown have tested the this method and compared it to the least-squares approach.[27,28] They reported that the accuracy of MEM analyses can exceed those based on least-squares fitting when the decay is measured with sufficient precision over the appropriate range of modulation frequencies. In the case of excited-state reactions between the sample components, fluorescence distributions cannot be recovered from the component decays because the decays of all the species that emit the same spectra are averaged, obscuring the structure of $\mathbf{W}$.

When the spectra fluorescing components are not known, the quantum yields or photoproduction rates typically will not be available either. Equation 9 can be rewritten to include the photon production rates as matrix components rather than spectral normalization factors:

$$\tilde{\mathbf{D}} = \mathbf{X}\tilde{\mathbf{Y}}' = \mathbf{A}\Psi\tilde{\mathbf{Y}}' \quad (18)$$

where $\mathbf{\Psi}$ is a diagonal matrix comprised of the component photon production rates. The matrix $\mathbf{A}$ is $\mathbf{X}$ normalized so that the sum of squares of each column is equal to 1. When the emission-frequency domain decay matrix is analyzed without regard to Ψ, the results are $\mathbf{A}$, $\mathbf{\Psi K \Psi}^{-1}$, and $\mathbf{\Psi y}_0$. As in the case of parametric decay analysis, the relative steady-state intensities are calculated by scaling the initial intensities, $\Psi\mathbf{y}_0$, by the component lifetimes. The component decay times (diagonal elements of $\mathbf{K}$) are unaffected by Ψ, but the rates of excited-state reactions (off-diagonal elements of $\mathbf{K}$) will be scaled by the ratios of component photon production rates. The production rate values can be constructed from literature or experimental values and used to adjust $\mathbf{\Psi K \Psi}^{-1}$ and $\mathbf{\Psi y}_0$ prior to further analysis or data interpretation.

Matrix Acquisition/Spectra Known. When the spectra of the mixture components are known, and the entire complex quantum yield matrix has been measured, the analyst can choose between two approaches to analyzing the component decays. In the first, the frequency domain decays of the components can be calculated directly from the decay matrix, $\tilde{\mathbf{D}}$ by linear regression of the spectral matrix. This is accomplished using the pseudoinverse of the spectral matrix, i.e.

$$\tilde{\mathbf{Y}}' = \mathbf{X}^+\tilde{\mathbf{D}} \quad (19)$$

A correctly normalized matrix $\mathbf{X}$ can be constructed by collecting all the standard spectra at a single concentration using a single instrument and dividing each standard spectrum by its respective lifetime. The photokinetic transfer matrix and initial intensities can be calculated from the frequency domain decays using eqs 6 and 7, respectively. When the spectra are correctly normalized, the columns of the matrix $\tilde{\mathbf{Y}}_0$ are proportional to the concentrations of the sample components.

The second approach to the analysis of decay matrices when the spectra are known is to use the standard spectra to constrain the partitioning of the matrix $\tilde{\mathbf{D}}$. This can be accomplished by incorporating a measure of the similarity of the transformed principal components to the standard spectra into the partitioning objective function vector. If $\tilde{\mathbf{D}}$ were a noise-free matrix, the results would be identical to the results of the multiplication in eq 19 within numerical limitations. Because of measurement errors, the standard spectra will not form a perfect basis set for the columns of $\tilde{\mathbf{D}}$. Consequently, the corresponding frequency domain decays will not be optimal either. Use of the standard spectra to constrain the spectral factors produces the factors that are consistent with the standard spectra, yet also meet as many of the other criteria for factors as possible. In this paper, the difference of the correlation matrices of the standard spectra and the transformed principal components was used as the similarity measure. The difference matrix is given by

$$\Delta_x = \mathbf{X}'\mathbf{X} - (\tilde{\mathbf{U}}\tilde{\mathbf{\Pi}})'(\tilde{\mathbf{U}}\tilde{\mathbf{\Pi}}) \quad (20)$$

Minimizing the elements of this difference matrix during the partitioning process maximizes the similarity of $\tilde{\mathbf{U}}\tilde{\mathbf{\Pi}}$ to $\mathbf{X}$. The frequency domain decay matrix is calculated using the inverse transform via eq 14. The photokinetic transfer matrix and initial intensities are calculated from the frequency domain decay matrix using eqs 6 and 7, respectively.

Acquisition at Selected Wavelengths. It is not necessary to measure the entire matrix $\tilde{\mathbf{D}}$ to carry out a decay analysis in the

(26) Reiter, J. *J. Comput. Phys.* **1992**, *103*, 169−183.
(27) Shaver, J. M.; McGown, L. B. *Anal. Chem.* **1996**, *68*, 9−17.
(28) Shaver, J. M.; McGown, L. B. *Anal. Chem.* **1996**, *68*, 611−620.

frequency domain. Theoretically, a submatrix of $\tilde{\mathbf{D}}$ aquired at selected wavelengths could be analyzed without a priori information using matrix partitioning. However, since it is impossible to validate the incomplete spectral profiles that would be generated, this approach would be unreliable. On the other hand, when the fluorescence emission spectra of the components are known, the frequency domain decay matrix, $\tilde{\mathbf{Y}}$, can be calculated from decays measured at selected emission wavelengths. Frequency domain decays measured at selected wavelengths constitute a subset of the rows of $\tilde{\mathbf{D}}$. This subset matrix is given by the equation

$$\tilde{\mathbf{D}}^{\subset} = \mathbf{X}^{\subset}\tilde{\mathbf{y}}' \tag{21}$$

where $\tilde{\mathbf{D}}^{\subset}$ denotes a subset of the matrix $\tilde{\mathbf{D}}$ and $\mathbf{X}^{\subset}$ denotes a subset of the spectral matrix $\mathbf{X}$. The elements of the subset matrices correspond to the complex quantum yields and component emission intensities measured at the r selected wavelengths. In order to preserve the concentration dependence of the intensities, the elements of this matrix should be taken from time-independent standard emission spectra. The frequency domain decays can be calculated from the regression of the decay submatrix using the spectral submatrix, i.e.

$$\tilde{\mathbf{Y}}' = (\mathbf{X}^{\subset})^{+}\tilde{\mathbf{D}}^{\subset} \tag{22}$$

The photokinetic transfer matrix and relative concentrations can be calculated from the frequency domain decays using eqs 6 and 7, respectively.

EXPERIMENTAL SECTION

Materials. In the measurements described here, the following reagents were used as received: benzo[*k*]fluoranthene (98%), fluoranthene (98%), benzo[*a*]pyrene (98%), 9-phenylanthracene (98%), 9-methylanthracene (98%), (Chem Service, West Chester, PA); benzo[*ghi*]perylene (98%) (Aldrich Chemical Co., Milwaukee, WI); *p*-bis[2-(5-phenyloxzoyl)]benzene (POPOP) (Exciton Chemical Co., Inc., Dayton, OH); and sodium dodecyl sulfate (99% purity, Sigma Chemical Co., Milwaukee, WI). Ethyl alcohol (absolute, 200 proof, Quantum Chemical Co., Tuscola, IN) was purchased at the highest available purity. Freshly prepared solutions were used for all measurements. Fresh PAH solutions were prepared for each measurement by dilution of stock solutions in ethanol. The PAH solutions in SDS micelles were prepared using aqueous SDS solutions which had been sonicated for at least 1 h in a bath sonicator (final temperature 45 °C) and cooled to room temperature prior to the dilution. Final ethanol concentrations in the SDS solutions were below 1%. All aqueous solutions were prepared using distilled−deionized water.

Absorbance Measurements. The absorption spectra of each standard and mixture solution was measured using an 8452A diode array spectrometer (Hewlett-Packard, Palo Alto, CA) prior to fluorescence measurements. The absorbance of all solutions was below 0.1 absorbance unit at the excitation wavelength.

Fluorescence Measurements. Steady-state and lifetime fluorescence measurements were acquired using a multifrequency cross-correlation phase-modulation spectrofluorometer (K2, ISS, Champaign, IL). Data acquisition was controlled by a 100 MHz 586 computer (Gateway, Bozeman, SD). Excitation at 363 nm was provided by a 6 W argon ion laser (Innova-90, Coherent, Santa Clara, CA). Steady-state spectra and single-wavelength decays were collected at 90° to the excitation, dispersed by a monochromator equipped with a 1200 groove/mm grating and 1 mm entrance and exit slits (H1061, Instruments SA, Metuchen, NJ), then detected by a blue-enhanced photomultiplier tube (R928, Hamamatsu, Bridgewater, NJ). The complex quantum yield matrix was calculated from fluorescence emission acquired at 90° to the excitation, dispersed by a spectrograph equipped with a 600 groove/mm grating (HR320, Instruments SA) and monitored using a 1024 element microchannel plate intensified photodiode array detector (IRY-1024, Princeton Instruments, Trenton, NJ). The lifetime data was acquired using POPOP in ethanol as the reference lifetime standard. The reference lifetime was assigned the widely accepted value of 1.35 ns.[29] Solutions were measured at ambient temperature and were not deoxygenated.

Data Analysis. All data analysis was performed on a SPARC 20 Unix workstation (Sun Microsystems, Palo Alto, CA) using software written by the author in MATLAB, an interactive programming language for matrix operations with graphics (The Mathworks, Natick, MA). The decay analysis code is based on the algorithm described here. The maximum entropy routine implementing the inverse Fourier and Laplace transforms is based on the algorithm of Reiter.[26]

The components of multichannel frequency domain decays are calculated from four measurements of the oscillating fluorescence intensity at a given excitation frequency. The oscillating fluorescence intensity is given by the expression

$$I_F(\lambda,t_k) = I_{DC}(\lambda) + I_{AC}(\lambda)\sin(\omega t_k + \phi) \tag{23}$$

where I_{DC} is the steady-state component of the oscillating signal and I_{AC} is the magnitude of the frequency dependent component. The measurement sampling times, t_k, are chosen so that the four measurements are evenly spaced during one oscillation period. The phase and modulation ($m = I_{AC}/I_{DC}$) can be calculated from the system given in eq 23 after expanding the oscillating term to $\sin(\omega t_k)\cos(\phi)$ by trigonometric identity. The intensity data was filtered using a second-order Butterworth low-pass filter prior to the calculation of the phase and modulation. The complex quantum yield matrix was calculated from the steady-state spectrum, phase, and modulation using eqn 10.

In traditional decay analysis, the χ^2 function is used to measure the goodness of fit of hypothetical kinetic models to experimental data. In model-independent analysis, the χ^2 function is used to evaluate the impact of measurement noise on the results. A refined version of the data matrix can be calculated using analysis results from which the components that can be attributed to noise, e.g., by sign, have been removed. The refined matrix is given by

$$\tilde{\mathbf{D}}_{ref} = \mathbf{X}_{real}\mathbf{W}_{ideal}\mathbf{\Gamma}_{real}\tilde{\mathbf{Z}} \tag{24}$$

where $\mathbf{X}_{real}$ is the real part of the spectral matrix, $\mathbf{W}_{ideal}$ is the identity matrix, $\mathbf{\Gamma}_{real}$ is a matrix that has the real components of the initial intensities along the diagonal (spectra and intensities calculated from experimental decays have small, but nonzero, imaginary coefficients), and $\tilde{\mathbf{Z}}$ is the matrix of the Fourier coefficients of pure ideal decays that have decay rates equal to the eigenvalues of $\mathbf{K}$. When the data quality is good and the decay

(29) Lakowicz, J. R.; Cherek, H.; Balter, A. *J. Biochem. Biophys. Methods* **1981**, *5*, 131−146.

is governed by a first-order kinetic equation, the χ^2 function comparing this refined matrix to the experimental data is small. In the case of the complex quantum yield matrix, the χ^2 function is given by

$$\chi^2_{\text{ref}} = \frac{1}{(p-1)(q-1)} \sum_{i=1}^{p} \sum_{j=1}^{q} \frac{(\tilde{d}_{ij}^{\text{exptl}} - \tilde{d}_{ij}^{\text{ref}})(\tilde{d}_{ij}^{\text{exptl}} - \tilde{d}_{ij}^{\text{ref}})^*}{\sigma_{ij}^2} \quad (25)$$

where σ_{ij}^2 is the variance of the complex quantum yield at each modulation frequency and wavelength combination and $(p-1)$-$(q-1)$ is the number of degrees of freedom associated with the variance of a $p \times q$ matrix.[30] The variance of the complex quantum yield is a function of the variances of the intensity, modulation, and phase shifts. The variance of a complex variable is the sum of the variances of the real and imaginary variable parts, which can be calculated using error propagation statistics. From eqs 3 and 4, the real and imaginary parts of the complex quantum yield are given by

$$d_{\text{real}}(\lambda,\omega) = x(\lambda)m(\omega)\cos(\phi(\omega)) \quad (26)$$

$$d_{\text{imag}}(\lambda,\omega) = x(\lambda)m(\omega)\sin(\phi(\omega))$$

The variance derived from these expressions is

$$\sigma_{\text{d}}^2(\lambda,\omega) = \sigma_{\text{real}}^2(\lambda,\omega) + \sigma_{\text{imag}}^2(\lambda,\omega)$$

$$= m^2(\omega)\sigma_{x_0}^2(\lambda) + x_0^2(\lambda)\sigma_m^2(\omega) + x_0^2(\lambda)m^2(\omega)\sigma_\phi^2(\omega) \quad (27)$$

where σ_{X0}, σ_m, and σ_ϕ denote the standard deviations of steady-state intensities, modulation ratios, and phase shifts, respectively. The steady-state intensities typically have values around 2000 counts while the modulation and phase vary between 0 and 1 and 0 and 2π rad, respectively. Typical standard deviations for measurements made using photomultiplier tubes are 2.5% counts and 0.002 and 0.007 rad for σ_{X0}, σ_m, and σ_ϕ, respectively. For the intensified photodiode array, typical standard deviations are 5% counts and 0.01 and 0.024 rad, respectively.

Since the autocorrelation coefficient of the decay residuals is used as a measure of the quality of hypothetical models to experimental data, the autocorrelation coefficient also can be used to compare the experimental data to the refined version of the data matrix calculated using model-independent analysis. The autocorrelation coefficient is the dot product of the normalized residuals with a frequency-shifted version of itself. Specifically, the coefficient is given by the expression

$$r_{\text{auto}} = \sum_{i=1}^{p} \sum_{j=1}^{q} \frac{(\tilde{d}_{ij}^{\text{exptl}} - \tilde{d}_{ij}^{\text{ref}})}{||\tilde{D}^{\text{exptl}} - \tilde{D}^{\text{ref}}||} \frac{(\tilde{d}_{i(j+1)}^{\text{exptl}} - \tilde{d}_{i(j+1)}^{\text{ref}})}{||\tilde{D}^{\text{exptl}} - \tilde{D}^{\text{ref}}||} \quad (28)$$

When the residuals are randomly distributed around zero, the value of the autocorrelation coefficient approaches zero. Large, systematic residuals lead to autocorrelation values approaching 1.

(30) Malinowski, E. R. *Factor Analysis in Chemistry*, 2nd ed.; Wiley: New York, 1991.

Table 1. Analysis of Single-Component Decay[a]

frequency	m	σ_m	ϕ	σ_ϕ
1.25	0.992	0.005	6.55	0.094
2.08	0.980	0.011	10.63	0.100
3.48	0.960	0.021	17.55	0.427
5.80	0.885	0.009	27.70	0.344
9.68	0.750	0.006	41.19	0.256
16.14	0.562	0.010	55.95	0.500
26.93	0.379	0.008	68.05	0.548
44.92	0.241	0.002	76.93	0.183
79.94	0.146	0.007	81.99	0.713
125.0	0.086	0.004	84.99	1.665

	FDA	NLLS
τ	14.54	14.48
χ^2	0.69	1.15
r_{auto}	0.31	

[a] FDA, frequency domain analysis; NLLS, nonlinear least-squares fitting: no. of fitting parameters $p = 1$; no. of data points $N = 20$. $\chi^2 = 1/(N - p - 1)[((m_{\text{expt}} - m_{\text{sim}})^2/\sigma_m^2) + ((\phi_{\text{expt}} - \phi_{\text{sim}})^2/\sigma_\phi^2)]$.

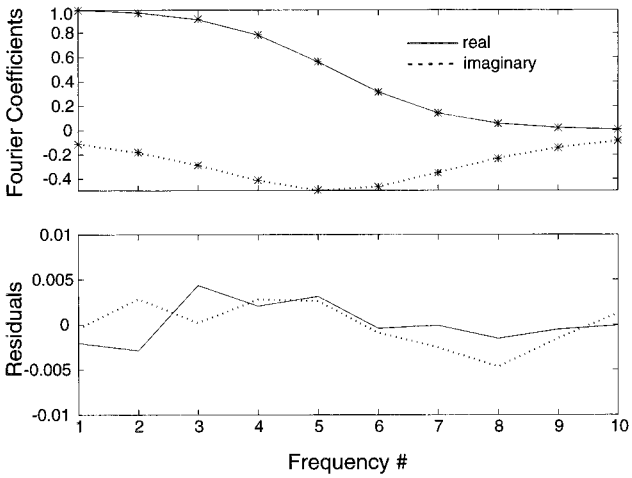

Figure 2. (A) Frequency domain decay of benzo[*a*]pyrene measured at 407 nm. (B) Residuals of idealized decay.

RESULTS AND DISCUSSION

Single-Component Decay. The phase angles and modulation ratios measured from the decay of a standard benzo[*a*]pyrene solution in ethanol at 407 nm using modulation frequencies between 1.25 and 125 MHz are listed in Table 1. The lifetime calculated from the normalized complex quantum yield is 14.55 ns. The standard deviations of the phase and modulation were measured at each frequency during the decay measurement. The deviation of the normalized complex quantum yield can be determined with eq 26 using $S_0 = 1$ and $\sigma_{S_0} = 0$. The χ^2_{ref} value of the decay is 0.69. The autocorrelation coefficient of the residuals is 0.31. The residual decay components are depicted in Figure 2. These data are all consistent with the recovery of a single lifetime from the decay data. The results of the analysis of this decay by nonlinear least-squares fitting are presented for comparison. The lifetime value obtained by nonlinear least-squares fitting is 14.48 ns with a χ^2 value (See legend Table 1.) equal to 1.15. These results are in excellent agreement, confirming the equivalence of the two approaches.

Table 2. Analysis of Simulated Multicomponent Decays[a]

simulation	spec corr	transfer matrix ($\times 10^{-7}$ s^{-1})		RSD		τ (ns)	$\Delta\tau$ (ns)	$I_F^\dagger$	$\Delta I_F^\dagger$	χ^2_{ideal}	χ^2_{ref}	r_{auto}
ideal	1.000	−21.44	1.2×10^{-3}	6.5×10^{-5}	0.115	4.665	−0.0004	na		na	na	na
Mat. Part.	1.000	2.0×10^{-5}	−6.99	1.240	2.2×10^{-5}	14.299	−0.0014	na				
PDA	0.999	−21.367	−0.040	0.003	2.189	4.680	0.015	na		0.75	0.60	0.18
Mat. Part.	0.997	0.011	−7.029	4.137	0.007	14.227	−0.073	na				
PDA	na	−21.275	−0.249	0.003	0.376	4.700	0.035	0.747	0.003	0.75	0.81	0.09
Mat Regr.	na	−0.076	−6.958	0.390	0.006	14.372	0.072	0.253	0.003			
PDA	na	−21.382	−0.014	0.003	1.536	4.677	0.012	0.748	−0.002	0.75	0.59	0.01
Con. Mat. Part.	na	−0.006	−7.002	9.414	0.006	14.271	−0.029	0.252	0.002			
PMT	na	−21.691	0.081	0.006	1.510	4.610	−0.055	0.749	−0.001	0.79	0.33	0.08
Submat. Regr.	na	0.018	−7.035	26.218	0.010	14.215	−0.085	0.251	0.001			
PMT (λerror)	na	−21.481	−0.047	0.005	3.260	4.655	−0.010	0.790	0.040	0.79	10.5	0.31
Submat. Regr.	na	0.994	−6.893	0.087	0.010	14.509	0.209	0.210	−0.040			

[a] Mat. Part., matrix partitioning; Con. Mat. Part., constrained matrix partitioning; Mat. Regr, matrix regression; Submat. Regr., submatrix regression; PDA, photodiode array; PMT, photomultiplier tube; na, not applicable.

Simulated Multicomponent Decays. A series of data matrices simulating the emission decay of a mixture of benzo[*a*]pyrene, and 9-methylanthracene was constructed via eq 9 using experimental emission spectra, simulated frequency domain monoexponential decays, and normally distributed random numbers. The first matrix, denoted "ideal", is noise-free. The second matrix, labeled "PMT" because it simulates photomultiplier tube acquisition, was constructed by superimposing normally distributed random errors on the ideal matrix. A subset of the PMT matrix was analyzed using the procedure for decays monitored at selected wavelengths. The third matrix was constructed in the same manner to simulate intensified photodiode array detection and is labeled "PDA". The PDA matrix was analyzed using the procedures for matrix acquisition. The results of these analyses are presented in Table 2.

The results of the analysis of the ideal matrix by partitioning are listed in the first row of Table 2. The spectra resolved from this matrix agree perfectly with the spectra used to simulate the matrix, but there are very small differences in the values of the transfer matrix, decay times, and relative fractional intensities. These deviations are the consequence of numerical limitations on the partitioning process. The most stringent termination criteria used in the analyses reported here lead to transformation matrix elements that agree with the ideal values to the fourth decimal place.

The results of the analysis of the PDA matrix by matrix partitioning (eq 12) are the second set of data listed in Table 2. The correlation coefficients of the spectra resolved from this matrix with the ideal spectra are very close to 1, indicating minimal distortion of the spectral profiles. However, there is a larger discrepancy in the values of the transfer matrix elements. The deviations in the transfer matrix elements are 2−3 orders of magnitude larger than the deviations produced by the partitioning of the ideal matrix. The practical consequence of this is that the dynamic range of kinetic rates that can be analyzed is reduced to ∼2 orders of magnitude by the measurement error. The deviations in the decay times are on the order of 0.1 ns, which is typically expected for decays measured using the photomultiplier tube. Negative off-diagonal transfer matrix elements can be unequivocally attributed to measurement errors because most reactions between excited-state components have positive rates. (Reactions between ground-state components have no effect on the photokinetic rates.) The low excitation rates and concentrations used in the measurements simulated here make it unlikely that quenching by excited-state components, which would have negative rate constants, would be observed. When positive off-diagonals are small and of the same order of magnitude as the negative off-diagonal elements, it is reasonable, though somewhat subjective, to attribute them to noise. A less subjective approach to evaluating the relative significance of the elements of **K** is to subject them to a bootstrap procedure. In most frequency domain decay measurements, 8−12 frequencies are measured per decade of lifetimes analyzed, so eq 5 typically represents an overdetermined system of linear equations. Ideally, the value of **K** should not be affected by deleting any one of these equations, i.e., frequency components. In practice, measurement noise leads to variations in the values of **K** as individual frequency components are deleted from the system of equations. The relative size of these variations can be used to distinguish off-diagonals associated with noise from those associated with photokinetic processes. The relative standard deviations of the off-diagonal elements of **K** of the PDA matrix are 3 orders of magnitude greater than those of the diagonal elements, clearly establishing the connection of both off-diagonal elements to measurement noise. Two χ^2 values are reported in Table 2. The first, labeled χ^2_{ideal}, was calculated using a variant of eq 24 in which the refined data matrix is replaced by the ideal data. This value is close to 1 as expected. The second, χ^2_{ref}, was calculated using eq 24 and is slightly smaller than χ^2_{ideal}. This indicates that a portion of the noise variance is correlated with the signal and incorporated into the principal components and refined results. The autocorrelation coefficient of the residuals is close to zero as expected for random residuals.

The next entry in Table 2 consists of the results of the analysis of the PDA matrix by spectral matrix regression. The off-diagonal elements of the transfer matrix are ∼1 order of magnitude larger than those observed in the matrix partitioning solution, but the diagonal elements are similar to those of the partitioning solution and lead to decay times that also are within 0.1 ns of the expected lifetimes. The relative standard deviations of the off-diagonal elements of **K** are only 2 orders of magnitude greater than those of the diagonal elements. This clearly indicates that the off-diagonals are derived from measurement error, but less emphatically than in the case of the partitioned solution. The knowledge of the component spectra permits the calculation of the relative intensities of the components. They agree with those calculated from the ideal data to within 1%, which indicates that these values were minimally affected by the measurement errors. The value of χ^2_{ref} is closer to 1 than in the matrix partitioning solution,

indicating that the refined solution differs more from the data matrix. The residual autocorrelation coefficient is also slightly smaller, indicating even more randomness in adjacent residual components.

The results of the analysis of the PDA matrix using constrained matrix partitioning are similar to the results of the unconstrained partitioning analysis, but the off-diagonal elements of the transfer matrix are reduced by ~50%. Moreover, both off-diagonals are negative and have large relative deviations. The photokinetic matrix is unequivocally diagonal. The deviations in the decay times and relative intensities are also smaller than those observed in the partitioning or regression solutions. The χ^2 and autocorrelation coefficient values are consistent with the improvement in the refined data associated with the decay time and intensity value estimates.

A subset of the PMT matrix was formed by extracting three rows corresponding to the three wavelengths used in the analysis of mixture 3 described below. The PMT submatrix was analyzed by regression of the spectral submatrix. The results of the analysis are presented in Table 2. The off-diagonal elements of the transfer matrix are similar in magnitude to those observed in the PDA matrix partitioning solutions and lead to decay times that are within the 0.1 ns deviation expected for data acquired at this precision. Because the relative standard deviations of the off-diagonal elements of **K** are 2−3 orders of magnitude greater than those of the diagonal elements, the off-diagonals can be attributed to measurement error. The relative intensities of the components agree with the ideal data to within than 1%. The value of χ^2_{ideal} is close to 1, and the residual autocorrelation coefficient is very small. The mixture decay is well analyzed under these circumstances.

The PMT submatrix was also used to investigate the effect of monochromator setting errors on the results of frequency domain analysis. The monochromator setting errors were simulated by using a subset spectral matrix in eq 22 which was deliberately constructed using rows of the spectral matrix corresponding to wavelengths 0.5 nm higher than those used to construct the subset data matrix. The results are listed in the last rows of Table 2. The effect of this error on the transfer matrix elements is quite dramatic: one of the off-diagonal elements of the transfer matrix is nearly the same order of magnitude as the diagonal elements. Moreover, the results of the bootstrap analysis are more ambiguous; the relative standard deviation of the large off-diagonal element of **K** is only 1 order of magnitude greater than those of the diagonal elements. The impact on the decay times observed was mixed: the 9-methylanthracene lifetime is within the expected range, but that of the benzo[*a*]pyrene is more than 0.2 ns larger than the expected value. The deviation in the relative intensities is close to 5%, which is much larger than observed in the other analyses. The χ^2_{ideal} value is close to 1 as expected, but the χ^2_{ref} value is very large, indicating that the discrepancies incorporated into the refined decay data by the monochromator setting errors produce large deviations from the experimental data. These deviations are also less random, as indicated by the comparative size of the autocorrelation coefficient.

The analysis of these simulated decays indicates that the partitioning methods, i.e., with and without the standard spectra, have a slight advantage over the computationally straightforward regression method. The off-diagonals of the resulting photokinetics transfer matrices are smaller, though the decay times do not appear to be affected. Additionally, both the χ^2_{ref} and autocorrelation coefficient values were smaller using the partitioning methods. This is what one might expect since the partitioning routine can search among similar solutions for one that meets several of the optimization criteria.

EXPERIMENTAL RESULTS

Panels A−D of Figure 3 depict the standard fluorescence emission spectra of the mixtures analyzed for this report. In general, there is substantial but incomplete overlap in the spectra of all these mixtures, and the lifetimes are distinct with the exception of mixture 2. The mixtures were chosen to illustrate the relationship of the various forms of frequency domain analysis to the number of wavelengths monitored and the amount of sample information available to the analyst. The decays analyzed also illustrate the impact of measurement errors and component response overlap on the results of frequency domain decay analysis.

The first mixture analyzed was a mixture of 9-phenylanthracene, benzo[*a*]pyrene, and benzo[*ghi*]perylene solubilized in 37.5 mM SDS solution. The emission decay of this mixture was analyzed by partitioning the complex quantum yield matrix into the spectra and frequency domain decays of the components. The matrix was measured between 380 and 460 nm using 20 logarithmically spaced modulation frequencies between 0.5 and 50 MHz. An isometric plot of the matrix is depicted in Figure 4. The first step in the analysis of this matrix is the determination of the number of spectral components contributing to the matrix variance, i.e., the pseudorank of the matrix. The pseudorank was analyzed using the autocorrelation coefficients of the matrix singular vectors[25] and by an algorithm developed for complex quantum yield matrices.[13] The number of fluorescent components in this mixture was determined to equal three. In the next stage of the analysis, self-modeling curve resolution was used to reconstruct the component spectra and frequency domain decays from the principal components of the matrix. The spectra resolved from the mixture 1 matrix are depicted in Figure 5A. The lifetimes of the three components, 79, 33, and 8.3 ns, were determined from the diagonal of the photokinetic transfer matrix. The photokinetic transfer matrix, transfer matrix relative variations, χ^2_{ref}, and autocorrelation coefficient determined by frequency domain analysis of the component decays are presented in Table 3. These results indicate that the mixture is noninteracting and the decay constants of all three components are well estimated by this approach.

Since mixture 1 is solubilized in a microheterogeneous solvent, it is possible that the fluorescence decays of the components are characterized by distributions of closely related lifetimes rather than discrete lifetime values. Since the photokinetic transfer matrix is diagonal, no excited-state reactions complicate the frequency domain decays of the components. Fluorescence distributions can be recovered from the component decays nonparametrically using the maximum entropy method. The fluorescence distributions recovered from the component decays are depicted in Figure 5B. The widths at half the maximum height of the distributions are listed in Table 3. The distributions are skewed and the smaller of the widths is reported. As expected, the decays are characterized by lifetime distributions that have widths which increase with the lifetime of the components. One might predict that these widths are inflated due the large measurement errors associated with the photodiode array. This

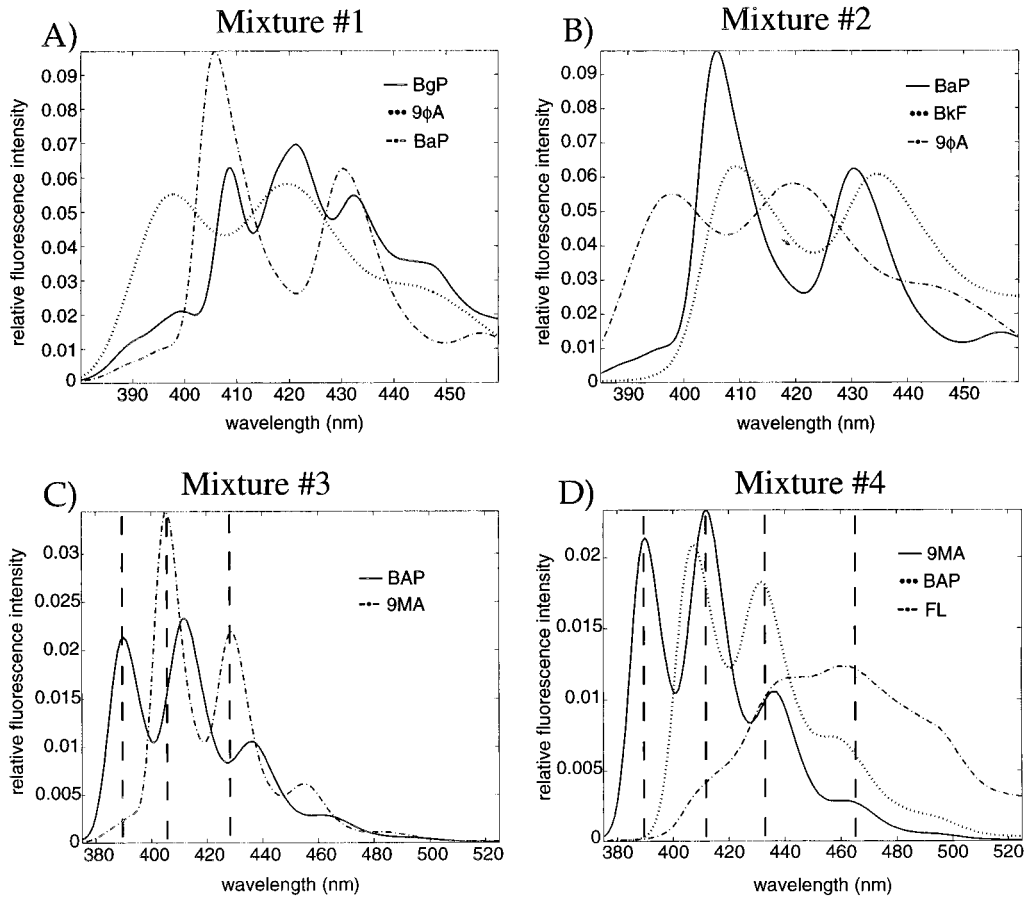

Figure 3. Compositions of the mixtures analyzed, fluorescence spectra, lifetimes, and quantum yields of mixture components. Dashed lines indicate wavelengths measured. (A) Mixture 1 in 37.5 mM sodium dodecyl sulfate: (---) 8.0×10^{-6} M 9-phenylanthracene ($\tau = 8.5$ ns; $\phi = 0.54$); (– · –) 1.67×10^{-6} M benzo[*a*]pyrene ($\tau = 34.1$ ns; $\phi = 0.59$); (—) 6.67×10^{-6} M benzo[*ghi*]perylene ($\tau = 82.9$ ns; $\phi = 0.28$). (B) Mixture 2 in 37.5 mM sodium dodecyl sulfate: (– · –) 8.0×10^{-6} M 9-phenylanthracene ($\tau = 8.5$ ns; $\phi = 0.54$); (---) 6.67×10^{-6} M benzo[*k*]fluoranthene ($\tau = 11.0$ ns; $\phi = 0.58$); (—) 1.67×10^{-6} M benzo[*a*]pyrene ($\tau = 34.1$ ns; $\phi = 0.59$). (C) Mixture 3, in ethanol: (—) 5.0×10^{-6} M 9-methylanthracene ($\tau = 4.7$ ns; $\phi = 0.21$); (– · –) 1.67×10^{-6} M benzo[*a*]pyrene ($\tau = 14.3$ ns; $\phi = 0.15$). (D) Mixture 4 in ethanol: (—) 1.0×10^{-6} M 9-methylanthracene ($\tau = 4.7$ ns; $\phi = 0.21$); (– · –) 5.0×10^{-7} M benzo[*k*]fluoranthene ($\tau = 8.0$ ns; $\phi = 0.54$); (---) 5.0×10^{-6} M fluoranthene ($\tau = 31.6$ ns; $\phi = 0.07$).

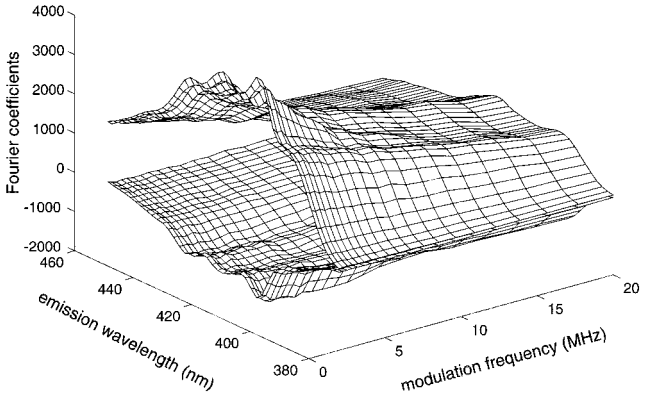

Figure 4. Isometric plot of the complex quantum yield matrix acquired from mixture 1. The positive elements are the real Fourier coefficients; the negative are the imaginary.

was confirmed by analyzing the decays of standards of the mixture 1 components in SDS solution measured on the photomultiplier tube using nonlinear least squares. The widths of the Gaussian lifetime distributions recovered from these decays also are listed in Table 3. The widths of the distributions recovered from the decays measured using the photomultiplier tubes are narrower than those of decays measured using the photodiode array, but the correlation between the lifetime and the width is still observed. Interestingly, the extent of the width inflation is not uniform.

The second multicomponent decay analyzed was acquired from a mixture of 9-phenylanthracene, benzo[*a*]pyrene, and benzo[*k*]-fluoranthene in 37.5 mM SDS solution (mixture 2). The decay matrix was measured between 380 and 460 nm using 12 logarithmically spaced modulation frequencies between 0.5 and 50 MHz. An isometric plot of the complex quantum yield matrix is presented in Figure 6. The decay of this sample is expected to be more difficult to resolve because the lifetimes of 9-phenylanthracene and benzo[*k*]fluoranthene are relatively close (8.5 and 11 ns, respectively), while the spectra of benzo[*a*]pyrene and benzo[*k*]fluoranthene are similar (see Figure 3B). The decay matrix was analyzed by spectral matrix regression using appropriately scaled emission spectra of the sample components. The results are presented in Table 3. The off-diagonals of the transfer matrix are as large as the diagonal elements, and there is little difference between the relative standard deviations of the diagonal and diagonal elements. The relative standard deviation of the benzo[*k*]fluoranthene decay rate is especially large. The lifetimes of the two extreme components, 9-phenylanthracene and benzo[*a*]pyrene, are much closer to the expected values than the intermediate lifetime component, benzo[*k*]fluoranthene, but none

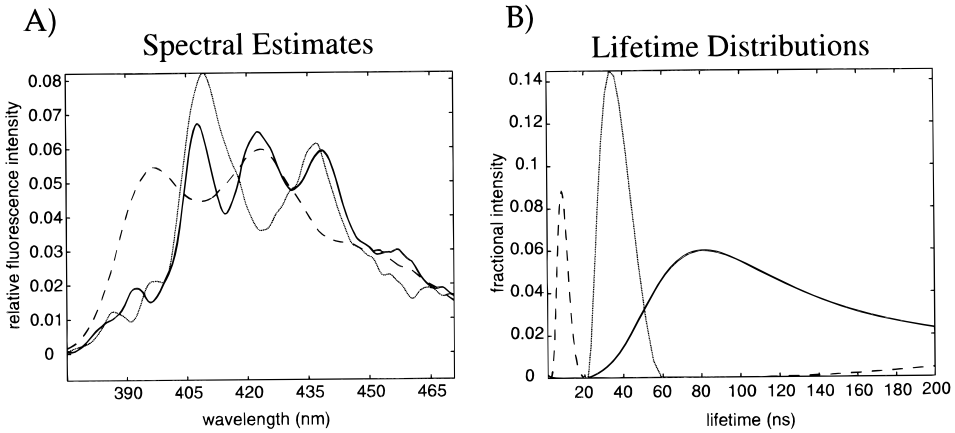

Figure 5. (A) Mixture 1 fluorescence emission spectra. (B) Mixture 1 lifetime distributions.

Table 3. Analysis of Experimental Multicomponent Decays[a]

mixture	transfer matrix ($\times 10^{-7}$ s^{-1})			RSD			τ (ns)	Δ_τ (ns)	δ_τ PDA	δ_τ PMT	$I_F^\dagger$	$\Delta I_F^\dagger$	χ^2_{ref}	r_{auto}
1, eq 16	−12.03	−0.07	−0.02	0.004	1.85	94.55	8.3	−0.2	±3.0	±0.4	na		1.12	0.06
	0.03	−2.95	−0.02	2.418	0.040	5.127	33.9	−0.2	±6.5	±6.5	na			
	−0.18	0.01	−1.26	0.174	6.73	0.036	79.3	3.6	±31.0	±16.4	na			
2, eq 14	−9.15	−3.30	0.74	0.013	0.079	0.098	10.9	2.4	na		0.111	0.000	72.3	0.58
	−3.54	−4.30	−0.67	0.284	0.118	0.138	23.3	12.3	na		0.370	−0.075		
	1.57	−1.76	−2.72	0.259	0.149	0.056	36.7	2.6	na		0.519	0.075		
2, eq 16c	−12.01	−0.16	−0.31	0.090	3.115	0.550	8.3	−0.2	±3.4	±0.4	0.105	−0.005	0.91	0.39
	0.83	−9.44	−0.84	1.995	0.278	0.550	10.6	−0.4	±5.6	±2.0	0.380	−0.065		
	0.105	−0.00	−2.59	12.71	14.21	0.054	38.6	4.5	±10.1	±6.5	0.515	0.070		
3, eq 13	−21.35	−0.56		0.004	0.102		4.68	0.02	na		0.745	−0.005	1.78	0.18
	0.450	−7.01		0.136	0.007		14.2	−0.04	na		0.255	0.005		
4, eq 13	−20.19	−5.00	0.04	0.015	0.198	1.981	4.95	0.28	na		0.828	0.043	1.47	0.11
	1.33	−13.40	−0.07	0.840	0.090	0.197	6.89	−1.11	na		0.043	−0.015	1.47	0.11
	1.33	−13.40	−0.07	0.840	0.090	0.197	6.89	−1.11	na		0.043	−0.015		
	−67.58	111.7	−3.27	0.250	0.211	0.021	30.5	−1.0	na		0.129	−0.028		

[a] na, not applicable.

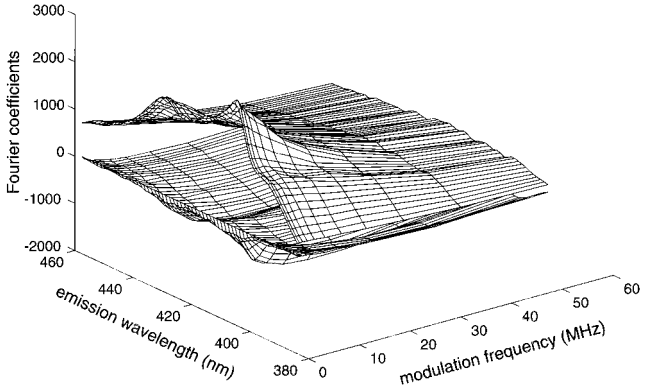

Figure 6. Isometric plot of the emission frequency domain decay matrix acquired from mixture 2. The positive elements are the real Fourier coefficients; the negative are the imaginary.

of the decay times is determined accurately. The relative concentration of 9-methylanthracene agrees with the expected value but those of the other two components differ by 7.5%. Due to the very large distortion of the benzo[*k*]fluoranthene lifetime, the χ^2_{ref} value is extremely large and the autocorrelation coefficient is much higher than that observed for the other decay analyses.

The size of the off-diagonals and relative standard deviations of the transfer matrix elements in the regression solution indicate that the result is unreliable. Therefore, mixture 2 was also analyzed using constrained matrix partitioning. The results of the analysis of this data matrix also are listed in Table 3. The results are a significant improvement over the regression solution. The off-diagonals of the transfer matrix have been reduced by nearly 1 order of magnitude, and their relative standard deviations have increased relative to the diagonal elements so that it is clear that the positive off-diagonals are produced by noise. The relative standard deviation of the benzo[*k*]fluoranthene decay rate is still much larger than that of the other components, but it is much smaller than the relative standard deviations of the positive off-diagonals. In fact, the relative standard deviations of the positive off-diagonals are 2−3 orders of magnitude larger than the diagonal elements. The overall accuracy of the component decay times also is increased by the constrained partitioning procedure although the benzo[*a*]pyrene lifetime is less accurate. The deviation in the relative concentrations was only slightly improved by the change in the analytical procedure. Since discrepancies of this magnitude are not observed in the quantitation of the samples measured on the photomultiplier tube, they may be related to the difference in the way the standard spectral matrix was constructed for photodiode array data. In an effort to match the signal intensities, the standard spectra were not measured using samples of equal concentration. So the deviation is most likely due to nonlinearity in the fluorophore signal as a function

of concentration on the photodiode array. The figures of merit indicate that the decay has been well analyzed: the χ^2_{ref} value is close to 1, and the autocorrelation coefficient is much less than 1. The autocorrelation coefficient is much larger than that observed for mixture 1, but it is similar to the value observed in the analysis of the single-component decay and consistent with random residuals.

The results of the analysis of mixture 3, a mixture of 9-methylanthracene and benzo[*a*]pyrene in ethanol, are listed next in Table 3. Emission decays were measured at 390, 405, and 430 nm (see Figure 3A) using 12 modulation frequencies between 5 and 50 MHz. The standard deviations of the phase and modulation were measured at each frequency during the decay measurement. The standard deviation of the steady-state intensity was found to be wavelength independent and equaled ∼2.0%. The observed lifetimes and relative concentrations are in excellent agreement with the expected values. The negative and positive off-diagonal elements of photokinetic transfer matrix are similar in magnitude, though they are somewhat larger than the off-diagonals observed in the analysis simulated PMT data. However, since the relative standard deviations of the off-diagonal elements are 2 orders of magnitude larger than those of the diagonal elements, the positive off-diagonal can be attributed to noise rather than an excited-state reaction. The relative fractional intensities are very close to the expected values. The value of χ^2_{ref}, though slightly higher than expected given the accuracy of the lifetimes and concentrations, is not substantially larger than 1. The autocorrelation coefficient is equal to 0.18, indicating random residuals.

The final set of results listed in Table 3 were recovered from a mixture of 9-methylanthracene, benzo[*k*]fluoranthene, and fluoranthene (mixture 4). This data set to illustrates the impact of low signal-to-noise ratio on the analysis results. Even though the concentrations are similar, the steady-state intensity of this mixture was ∼5 times smaller than that of mixture 3. The mixture decays were measured at 390, 410, 435, and 465 nm using 12 modulation frequencies between 2 and 25 MHz. The standard deviations of the phase and modulation were measured at each frequency during the decay measurement. The standard deviation of the steady-state intensity was found to equal ∼2.5% of the steady-state intensity. The observed lifetimes are within ∼1 ns of the expected values, but all of them have deviations that are significantly larger than the 0.1 ns typically associated with decay times determined using photomultiplier tubes. There are several large off-diagonal elements in the photokinetic transfer matrix, but most of them are negative. The variation in the off-diagonals identifies the one large positive off-diagonal in the transfer matrix as noise derived. The deviations in the fractional steady-state intensities of the benzo[*k*]fluoranthene and fluoranthene decays are slightly larger than those observed in the case of mixture 3 or the simulated PMT data, but they all agree to within 5%. The χ^2_{ref} value is only slightly larger than 1, and the residual autocorrelation coefficient indicates random residuals.

CONCLUSIONS

The decays of standards and mixtures of polynuclear aromatic hydrocarbons have been analyzed without fitting by multivariate analysis of the frequency domain decays of the sample components. The frequency domain analysis was applied to decays of mixtures measured at selected wavelengths, by using the fluorescence emission spectra of the mixture components to calculate the frequency domain decays of the components from the measured decays. Frequency domain decays were recovered from complex quantum yield matrices by regression using the spectra of the components and by a principal components analysis-based partitioning procedure. Fluorescence lifetime distributions were recovered nonparametrically from the decay of compounds in microheterogeneous solutions by using the maximum entropy method. These results indicate that it is possible to analyze fluorescence decays without fitting in the frequency domain. An additional benefit of this approach is that the analysis can generate the entire photokinetic transfer matrix, which includes the rates of excited-state reactions between the mixture components, when the signal-to-noise ratio of the data is sufficient.[13]

A series of analytical procedures for multicomponent decays measured under a variety of circumstances were described. Several procedures for characterizing analysis results were also described. The results indicate that the principal component-based partitioning procedures are superior to linear regression for more challenging analyses, i.e., decays of dilute or weakly emitting fluorophores or decays comprised of overlapping components. This procedure can be applied to the analysis of decays measured at selected wavelengths or across the entire emission spectrum. Moreover, the partitioning procedure is the only alternative when the component spectra are not known prior to the analysis. In order to determine the relative concentrations, the emission spectra of the components, including their relative rates of absorption and emission, must be known. Measurement errors pose significant limitations to the analysis of multicomponent decays, particularly in the case of widely differing decay rates and overlapped component decays. The results presented here indicate that the off-diagonals of the transfer matrix are significantly distorted when recovered from low SNR decays, complicating the interpretation of photokinetic transfer matrices in these cases. Decay times and relative concentrations are not distorted to the same extent. The development of improved signal acquisition and processing methods will greatly improve the analysis of such decays.

Received for review March 25, 1997. Accepted September 29, 1997.[⊗]

AC9703212

[⊗] Abstract published in *Advance ACS Abstracts*, November 15, 1997.